




Research Article

Iron ore mining areas and their reclamation in Minas Gerais State, Brazil: impacts on soil physical properties



Saulo Saturnino de Sousa¹ · Diego Antônio França Freitas¹ · Anderson Oliveira Latini¹ · Bruno Montoani Silva²  · João Herbert Moreira Viana³ · Matheus Pena Campos¹ · Devison Souza Peixoto² · Yves-Dady Botula⁴

Received: 4 May 2020 / Accepted: 27 August 2020 / Published online: 9 September 2020
© Springer Nature Switzerland AG 2020

Abstract

Plant cover acts to maintain the balance between soil chemical, physical, and biological attributes, as well as superficial soil protection. The aim of this study was to evaluate the impacts of iron ore mining and their reclamation on soil physical properties and soil visual quality in Fort Lauderdale Municipal Park and Serra do Curral Municipal Park, Iron Quadrangle (Quadrilátero Ferrífero), Minas Gerais State, Brazil. The evaluated areas varied in relation to the post-mining condition, natural revegetation (NR), an area with gully erosion (GA) and area under eucalyptus revegetation (ER) and native vegetation cover, rupestrian field (RF), and seasonal semi-deciduous forest (NF). The main soil physical attributes evaluated were: soil organic matter (SOM), geometric mean diameter (GMD), weighted mean diameter (WMD), bulk density (Bd), air capacity (ACb), plant-available water capacity (AWC), relative field capacity (RFC), and visual soil quality assessment. In addition to the impacts on the landscape, with removal of vegetation and soil cover, iron ore mining process impacts soil physical quality measured through porosity and aggregation properties and therefore could impact ecosystems services. Areas of iron post-mining that are not restored can develop gully erosion. NR shows high erosion risk inferred through aggregation indicators (GMD = 3.84 mm; MWD = 3.04 mm), despite similar soil organic matter content and higher plant-available water and air (NR [AWC = 0.102 m³ m⁻³; ACb = 0.328 m³ m⁻³], NF [AWC = 0.062 m³ m⁻³; ACb = 0.202 m³ m⁻³]) compared with NF (GMD = 4.77 mm; MWD = 4.56 mm). ER had similar soil structure stability compared to NF as well most of the porosity indicators, which is associated with the higher soil organic matter. Soil visual assessment alone was not able to characterize the soil physical quality, mainly in the post-mining areas, because it was designed for agricultural soils.

Keywords Land degradation · Mining area · Soil health · Environmental assessment · Iron Quadrangle

1 Introduction

Surface mining has a significant effect on the environment, such as vegetation removal, removal of soil, sediment exposure, water erosion, reduction of biodiversity, and contamination of soil and water resources [1–3], thereby significantly disturbing ecosystems [4].

Establishment of vegetation is a critical step in achieving the goal of ecosystem restoration in mining areas [3]. Particularly, iron ore mining impacts the landscape, since all vegetation and topsoil should be removed prior to excavation to reach iron ore deposits [4]. Effects on soil cover, and the difficulties in its restoration, are constantly reported [5]. Soil digging operations, detonations, and

✉ Bruno Montoani Silva, brunom.silva@ufla.br | ¹Programa de Pós-Graduação em Ciências - PPGCA, Universidade Federal de São João Del Rei - UFSJ, Campus Sete Lagoas - CSL, Rodovia MG 424 - Km 47, Sete Lagoas - MG CEP 35701-970, Brazil. ²Departamento de Ciência do Solo, Universidade Federal de Lavras - UFLA, Campus Universitário, Caixa Postal 3037, Lavras - MG CEP 37200-900, Brazil. ³Centro Nacional de Pesquisa em Milho e Sorgo - CNPMS, Empresa Brasileira de Pesquisa Agropecuária - Embrapa, Rod MG 424 Km 45, Zona Rural, Sete Lagoas - MG CEP 35701-970, Brazil. ⁴Research Institute on Mines and Environment, University of Quebec in Abitibi-Temiscamingue, Québec, Canada.



compaction caused by the weight of machines, among others, generate large quantities of residues [4]. These activities may cause direct and indirect negative effects [6]—chemical, biological, physical, structural, and aesthetic changes—depending on the origin material, geology, physical and chemical factors, vegetation, adopted management, and type of extracted material [7].

The method of reclamation depends on the scale of surface of mining impact, as well as on mining technology, intensity of disturbance, soil chemical and physical characteristics, and hydrological patterns [8]. In general, post-mining areas are highly compacted because of repeated movement of heavy equipment and rock fragments [1]. Compacted post-mining areas, due to the higher soil bulk density, have low soil porosity, resulting in limited water retention and nutrients uptake, which restricts root development [1, 9, 10]. In addition to the impact on soil physical properties, mining activities also cause drastic loss of soil organic carbon [1, 11, 12], thereby affecting in soil health and ecosystems services [13].

Soil is a good environment stratifier; therefore, an indicator of environmental quality can affect ability to keep the environment in balance [4]. Hence, monitoring of soil physical, chemical, and biological attributes is critical for assessing mining impacts and reclamation process [14]. Ultimately, combining laboratory-based and soil visual evaluation approaches has been advantageous for land management [15]. Visual soil assessment (VSA) is an approach based on visual properties allowing rapid assessment of soil quality [16], indicated to identify and improve the management systems and environmental preservation [17].

Mining is the most important economic activity of Minas Gerais State, in addition to tourism, metallurgy, and steel production [18, 19]. This region occupies approximately 7,000 km² and is mountainous, with altitudes of 1,000 to 2,000 m. The vegetation is relatively heterogeneous, including seasonal semi-deciduous forest, the transition between forest and “Cerrado” (Brazilian savanna), “Campos Cerrados” (savanna field), and “Campos Rupestres” (rupestrian field). Its hydrographic network is made up of two basins: the São Francisco River and the Rio Doce. Given the importance of the iron ore mining activity in the Minas Gerais State and the soil physical quality in the reclamation of these environments, studies need to be conducted to evaluate its effects on soil physical quality. Studies focusing on the soil physical quality recovery of high-altitude mining fields are scarce [20]. This is particularly the case with iron ore areas in tropical soils.

The hypothesis of this study is that different management conditions after iron ore mining will promote differences in soil physical quality and visual soil analysis. The aim of this study was to evaluate the impacts of iron ore

mining and their reclamation on soil physical properties in Fort Lauderdale Municipal Park and Serra do Curral Municipal Park, Minas Gerais State, Brazil. Also, we tested the VSA as a quick and easy method to assess soil quality.

2 Materials and methods

2.1 Description of the study area and sampling

The studied areas are in the Serra do Curral and Fort Lauderdale Municipal Parks, which are part of the Serra do Curral complex, in the Iron Quadrangle, located in Belo Horizonte, Minas Gerais State, Brazil (Fig. 1). This region is located between the coordinates 19°57'41.98" S and 43°55'12.30" W. The climate is classified as Cwb, according to Köppen's climate classification [21], and the dominant pedological units are associations between Entisols and Inceptisols [22].

The studied areas varied in relation to the post-mining condition and native vegetation cover. The post-mining areas had their surface layer and vegetation removed for iron ore extraction. Following the completion of iron ore mining, some 36 years ago, an area under natural revegetation (NR), an area that suffered an erosion process culminating in a gully (GA), and another that received eucalyptus revegetation (ER) were selected. Near the studied areas, there are active mines and others are closed mines. Two areas with distinct native vegetation were used as reference condition: rupestrian field (RF) and seasonal semi-deciduous forest—native forest (NF).

The RF is a phytophysognomy which occurs mainly on the mountains of the Southeastern, Central, and Northeastern Brazil, usually above 900 m altitude [23]. It shows a random distribution with shallow soils and rocky outcrops [24]. The RF vegetation contains many endemic species, adapted to large temperature variations and low water availability, acid soils, and fire occurrence [23]. Seasonal semi-deciduous forests are tropical forests that are subjected to a well-defined dry season, in which a portion of the trees lose their leaves. They are part of the Atlantic Forest Biome [25], which is a biodiversity hot spot for conservation priorities [26].

The NR, ER, and RF are under Entisols, GA under exposed saprolite, and NF under Inceptisol. All areas are hilly relief and geological material of itabirites and quartzites. The NR and RF areas are covered with grasses and small spaced shrubs, characteristic of rupestrian fields.

Soil sampling was carried out at random in the areas in order to represent the different post-mining conditions and the two areas with native vegetation. The five areas were sampled, with five replicates, collected in the 0.0–0.10 m layer for undisturbed samples. Undisturbed

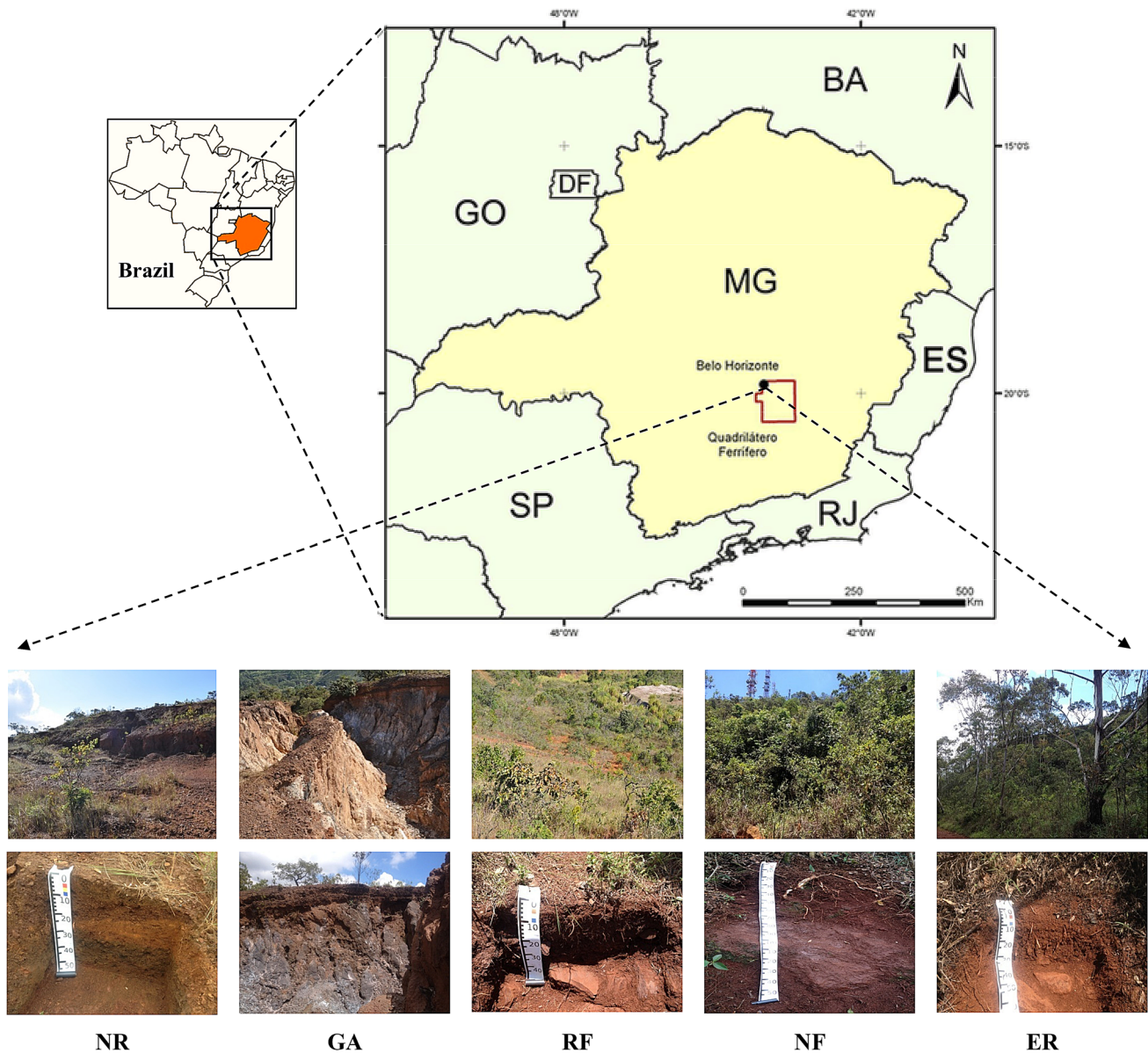


Fig. 1 Location of the areas affected iron ore mining and native vegetation in Iron Quadrangle, Minas Gerais State, Brazil. NR=natural revegetation; GA=gully area; RF=rupestrian field; NF= native forest; and ER=eucalyptus revegetation

samples were taken with the Uhland sampler [27], using steel cylinders with height and pre-measured diameters. Aggregate and disturbed samples were also collected by clods taken at two depths, 0.0–0.10 and 0.10–0.20 m in small trenches of 0.40 × 0.30 m (Fig. 1).

The soil texture analysis was determined by the pipette method in a dry air sample (< 2 mm), using NaOH dispersion (0.10 mol L^{-1}) and slow stirring (40 rpm) for 16 h. Total clay (< 0.002 mm), silt (0.05–0.002 mm), and sand (0.05–2 mm) were quantified (Table 1). The procedure was repeated without the addition of NaOH for quantification of the water dispersible clay (WDC) and calculation of the

flocculation index (FI). Stoniness of the soil, visually very prominent in the area, was evaluated by sieving (> 2 mm). Soil organic matter (SOM) was determined by oxidation of the organic matter with $\text{K}_2\text{Cr}_2\text{O}_7$ in a sulfuric medium. The procedures followed the protocols described by Teixeira et al. [28]. The chemical characterization of the soil at the time of sampling and the results of the textural analysis are presented in Tables 1 and 2.

Table 1 Clay, silt, and sand content for two soil layers in areas affected by iron ore mining and native vegetation in the Serra do Curral Municipal Park and Fort Lauderdale Park, Minas Gerais State, Brazil

Site	Clay	Silt (%)	Sand
<i>0.0–0.10 m depth</i>			
NR	40	47	13
GA	17	54	29
RF	28	46	26
NF	9	62	29
ER	33	24	43
<i>0.10–0.20 m depth</i>			
NR	45	39	16
GA	23	47	30
RF	29	47	24
NF	10	59	31
ER	24	37	39

NR natural revegetation; GA gully area; RF rupestrian field; NF native forest; ER eucalyptus revegetation

2.2 Indicators of soil structure stability

To determine the soil aggregates stability, we used aggregates of 8 to 4 mm diameter. After pre-wetting, these were submitted to wet sieving [28], through sieves: 2.0 mm, 1.0 mm, 0.5 mm, 0.25 mm, and 0.09 mm, to separate size classes of aggregates. Stirring was performed at 10 rpm for 15 min. In addition, the geometric mean diameter (GMD), the weighted mean diameter (WMD), the aggregate stability index (ASI) [29, 30], and the structural stability index (SSI) [31] were calculated. For the calculation of SSI, the following equation was used:

$$SSI = \frac{1.72 \text{ SOM}}{(\text{silt} + \text{clay})} \times 100$$

where SOM is the content of soil organic matter (% by mass), and silt + clay is the added content of silt and clay in the sample (% by mass).

For the calculation of ASI, the following equation was used:

$$ASI = \frac{\text{drp} - \text{wp25} - \text{Sand}}{\text{drp} - \text{Sand}}$$

where drp is the dry sample weight, wp25 is the weight of the class aggregates < 0.25 mm and Sand is the weight of the sand fraction of the soil sample.

2.3 Indicators of soil porosity

To obtain the soil water retention curve, the samples were weighed after being saturated with distilled water by capillarity for 48 h. Then, they were subjected to matric potentials of – 10, – 20, – 40, – 60, – 80, – 100, – 330, – 100

0, – 5000, and – 15,000 hPa. The automated tension table (ECOTECH) was used for matric potential of up to – 100 hPa and the other matric potential reached in Richards' Chamber (SOILMOISTURE EQUIPMENT CORP.) of mean and high pressures.

The bulk density (Bd) was determined by the volumetric ring method and the particle density (Pd) by the volumetric flask method according to Teixeira et al. [28]. The total porosity (TP) was determined by the water content in saturated condition. The pore size distribution was determined having a border diameter of 0.05 mm, obtained by water content equilibrium at – 60 hPa for separation of macroporosity (Mac) and microporosity (Mic) [32].

The water retention curves were adjusted to the van Genuchten [33] model with Mualem restriction [$m = 1 - (1/n)$]. Field capacity (FC) was estimated by equilibrium water content at – 100 hPa [31, 34]. The permanent wilting point (PWP) was estimated by equilibrium water content at – 15,000 hPa. The plant-available water capacity (AWC) of the soil was calculated by the difference between the FC and PWP.

The bulk air capacity (AC_b) indicates soil's air-holding capacity [31] and was obtained by the equation:

$$AC_b = TP - FC$$

The relative field capacity (RFC) represents the soil's capacity to store water and air in relation to the total porosity [35] and is obtained by the equation:

$$RFC = \frac{FC}{TP}$$

The soil water content at the inflection point (θ_{INFL}) was obtained by the equation presented by Dexter and Bird [36] from the soil water retention curve modeled by van Genuchten [33], as follows:

$$\theta_{INFL} = (\theta_{sat} - \theta_{res})(1 + 1/m) - m + \theta_{res}$$

where θ_{sat} is the water content in a saturated sample; θ_{res} is the water content at matric potential – 15,000 hPa, and m is a parameter of model adjustment.

The θ_{INFL} has been associated with water content in FC in tropical soils due to high correlation with in-field method [37, 38]. Thus, its use in the calculation of AWC was also evaluated using θ_{INFL} , obtained by:

$$AWC_{INFL} = (\theta_{INFL} - \theta_{PWP})$$

The SAWCa software [39] was used to calculate the S Index, the slope of water retention curve at the inflection point [40], and the integral energy (E_i) required for soil water extraction in the soil moisture range delimited by the AWC, according to methodology recommended by Asgarzadeh et al. [39].

Table 2 Chemical properties of the soil samples in two soil layers in areas affected by iron ore mining and native vegetation in the Serra do Curral Municipal Park and Fort Lauderdale Park, Minas Gerais State, Brazil

Site	pH (-)	K (mg dm ⁻³)	P (mg dm ⁻³)	Ca (cmol _c dm ⁻³)	Mg (cmol _c dm ⁻³)	Al (cmol _c dm ⁻³)	H+Al (cmol _c dm ⁻³)	t	T (cmol _c dm ⁻³)	BS (%)	M (%)	P-rem (mg L ⁻¹)
0.0–0.10 m												
NR	5.10	36.00	1.71	1.70	0.30	0.10	6.30	2.19	8.39	24.94	4.57	13.75
GA	5.70	34.00	1.42	0.40	0.10	0.10	2.59	0.69	3.18	18.46	14.49	34.07
RF	6.30	44.00	2.60	2.30	0.50	0.10	2.90	3.01	5.81	50.13	3.32	25.81
NF	4.40	26.00	3.53	0.50	0.10	0.70	19.15	1.37	19.82	3.36	51.09	15.49
ER	4.70	58.00	10.64	1.10	0.30	0.40	12.28	1.95	13.83	11.20	20.51	15.94
0.10–0.20 m												
NR	5.50	30.00	1.13	0.60	0.10	0.10	3.62	0.88	4.4	17.66	11.36	12.53
GA	5.20	12.00	0.84	0.10	0.10	0.10	3.24	0.33	3.47	6.65	30.30	24.34
RF	6.10	18.00	1.42	0.80	0.10	0.10	2.32	1.05	3.27	28.93	9.52	13.75
NF	4.60	36.00	3.53	0.40	0.10	0.90	19.15	1.49	19.74	3.00	60.40	13.33
ER	5.30	56.00	6.85	1.10	0.30	0.30	7.04	1.84	8.58	17.99	16.30	17.86

pH = pH in water; K = potassium; P = phosphorus; Ca = calcium; Mg = magnesium; Al = aluminum; H+Al = potential acidity; t = cation exchange capacity in actual pH; T = cation exchange capacity in pH 7.0; BS = Base saturation; m = aluminum saturation; P-rem = reminescent phosphorus; NR = natural revegetation; GA = gully area; RF = rupestrian field; NF = native forest; ER = eucalyptus revegetation

2.4 Visual soil quality assessment

Three visual evaluations were performed in each area, according to Niero et al. [17], with the procedures of Shepherd [16]. For each attribute, a score ranging from 0 to 2 (with fractions) was given: 0 (poor), 1 (moderate), and 2 (good), by comparison with the photographs in the author's field guide.

Visual evaluation of the soil structure was based on the side analysis of a "clod" of approximately 0.20 m. The clod was dropped into a plastic tray, from a height of 1 m, up to three times, if there was no disaggregation after previous drops. The coarse and fine fractions were moved to opposite ends of the tray, thus obtaining a gradient of size compared to the photographs in the field manual. The color and presence of mottling were evaluated in the same clod. The visual porosity was evaluated by the exposure of the face originating from the separation of structural units, compared to the manual's photographs. The plant cover assessment was made from the observation of dead cover and plant residues on the surface of the soil. The surface relief evaluation was assessed by the difficulty of transit over the area compared to that described in the manual.

To evaluate the soil quality index, each attribute received a score and a weighting of its importance, according to the methodology described by Shepherd [16]. The sum of the values obtained with the weighting classified the soil as: poor (sum less than 10), moderate (sum between 10 and 25), or good (values greater than 25).

2.5 Data analysis

Principal component analysis (PCA) was used to determine the soil physical properties that most differentiated the sampled areas. These attributes consisted of dependent variables for the null hypothesis tests of equality of parameters among regions, using a *one-way* ANOVA model. The *a priori* tests, *Shapiro–Wilk* and *Levene*, were carried out to investigate the assumptions. When there was no normality and/or homogeneity of variances by the *Shapiro–Wilk* and *Levene* tests, a *Box–Cox* transformation was performed to obtain it. The *Tukey* test was used in the *posteriori* tests for soil physical properties and *Scott–Knott* test for visual soil assessing, using the 5% level of significance. The analyses were performed using the R software 3.6.1.[41].

3 Results and discussion

3.1 Soil aggregate stability

There was no significant effect of the sampling depth (0.0–0.10 m and 0.10–0.20 m) or the interaction between

Table 3 ANOVA tests (*F* values) and/or Kruskal–Wallis (*H* values) for soil physical properties in areas affected by iron ore mining and native vegetation in the Serra do Curral Municipal Park and Fort Lauderdale Park, Minas Gerais State, Brazil

Variable	Sites				
	GA	NR	RF	ER	NF
GMD, mm	3.09d	3.84c	4.09cd	4.64ab	4.77a
MWD, mm	1.75c	3.04b	2.84b	4.33a	4.56a
SSI* (%)	1.11b	4.07ab	5.03a	6.74a	7.36a
ASI* (%)	53.52c	93.74ab	82.14bc	96.91a	97.86a
SOM* (%)	0.80b	3.34a	3.60a	4.22a	5.09a
Bd (Mg m ⁻³)	1.51ab	1.41a	1.54ab	1.70bc	1.93c
TP (m ³ m ⁻³)	0.463bc	0.579a	0.532ab	0.473bc	0.454c
Mac (m ³ m ⁻³)	0.209ab	0.298a	0.159b	0.221ab	0.227ab
RFC	0.549ab	0.479b	0.672a	0.511ab	0.488ab
AC _b (m ³ m ⁻³)	0.212b	0.328a	0.280ab	0.220 b	0.202b
AWC (m ³ m ⁻³)	0.120b	0.102b	0.156a	0.061c	0.062c
AWC _{INFL} (m ³ m ⁻³)	0.211ab	0.293ab	0.311a	0.239ab	0.192b
θ _{INFL} (m ³ m ⁻³)	0.360bc	0.442ab	0.460a	0.387abc	0.341c
S Index	0.065a	0.071a	0.063ab	0.044ab	0.034b
Stoniness (%)	51a	66ab	71ab	88b	78b

Means followed by the same letter in the row do not differ at the 5% level of significance by the *Tukey* test. *Medians followed by the same letter do not differ at the 5% level of significance by the *Kruskal–Wallis* test. MWD: mean weighted diameter; GMD: geometric mean diameter; SSI: structural stability index; ASI: aggregate stability index; SOM: soil organic matter; Bd: bulk density; TP: total porosity; Mac: macroporosity; RFC: relative field capacity; AC_b: air capacity; AWC: available water capacity; AWC_{INFL}: available water capacity at the inflection point; θ_{INFL}: water content at the inflection point; NR=natural revegetation; GA=gully area; RF=rupestrian field; NF=native forest; ER=eucalyptus revegetation

area and depth ($p > 0.05$) for soil properties MWD, GMD, SSI, and ASI, except for SOM. Thus, the mean values for the 0.0–0.20 m layer are presented (Table 3).

The reference area for comparing the impacts of iron ore mining on soil physical properties is the RF, as it is in the same type of soil (Inceptisol) as the mined areas. The greatest impact of mining on the attributes of soil aggregation and SOM was in the area where the most intense erosive processes were observed (GA). In areas with some revegetation process, it was possible to recover some soil physical properties. The ER was able to improve some attributes of soil aggregation, such as GMD, MWD, and ASI. This result may have been driven by the application of fertilizers in the implantation and conduction of eucalyptus, as can be seen by the higher levels of *P* and *K* (Table 2). Therefore, eucalyptus revegetation in post-iron ore mining areas is a good technique for recovering soil physical properties.

The GA had the lowest values of MWD, GMD, SSI, ASI, and SOM. NR and RF had intermediate values, while ER and

NF had the highest soil aggregation indexes (Table 3). Soil aggregation is a good indicator of soil quality influenced by different land uses [42–44]. SSI below 5% indicates high impact, between 5 and 7% indicates a high risk of structural degradation, and above 7% indicates low risk of degradation [45]. Only the NF had an SSI greater than 7%, indicating that the soils of the areas under reclamation, and even the RF, present high risk of loss organic carbon and susceptibility of soil erosion.

SOM was lower in GA, and among the other areas, there was no difference (Table 3). The SOM is closely related to all soil physical attributes [46], acting in all phases of the aggregation process, conferring greater stability to them by composing and stabilizing even macroaggregates. Thus, SOM is important to maintain good physical soil quality and strongly affects environmental quality [47, 48]. Continuous gully erosion has a significant effect on soil erodibility, and the parent material exposed on the soil surface shows very low aggregate stability [49]. This low aggregate stability increases soil erosion, and intensive erosion inhibits the development of stable soil profiles.

Reforestation affects the stabilization of degraded mining soils in several ways. The physical effect of roots on soil structure stability by enmeshing soil particles and chemical through releasing root exudates [50, 51], increases the soil cover's resistance to erosion, which accelerates as the accumulation of soil organic matter and biological process. Beneficial changes in physical, chemical and biological properties and processes increased aggregate stability of reforested topsoils [11, 49, 52].

Therefore, post-mining areas where care is not taken against intense erosive processes (GA) showed less SOM and aggregate stability, while the area that was reclaimed with eucalyptus (ER) presented SOM and aggregate stability similar to the native forest, and greater than the naturally revegetated area.

3.2 Soil porosity and plant-available soil water capacity

The B_d values were higher in the NF (1.93 kg dm^{-3}) and lower in the GA (1.51 kg dm^{-3}), NR (1.41 kg dm^{-3}), and RF (1.54 kg dm^{-3}). This is due to higher P_d and soil stoniness in the NF, therefore, due to the soil characteristics, and not by the post-mining vegetation cover. Mining can cause an increase in B_d due to compaction of the heavy traffic and drastic loss of SOM [1], which was not observed in this study. TP, Mac, and ACb were higher in NR and lower in NF and RF (Table 3). Mac and ACb values are higher than those considered critical ($< 0.100 \text{ m}^3 \text{ m}^{-3}$) in the literature [53]. The RFC was higher in the RF and lower in the NR. The RFC indicates the soil's ability to store water and air relative

to the soil's total porosity. Lower RFC values ($\text{RFC} < 0.6$) indicate a soil with water limitation, and greater RFC values ($\text{RFC} > 0.7$) indicate soil with limited aeration [35]. Except for the RF area with a RFC in the optimal range, the other areas have soils with water limitation (Table 3). Therefore, the biggest limitation of soils in the studied areas was the low water availability, especially due to the low clay content and high stoniness.

The S Index was higher in the GA and NR areas and lower in the NF area. The S Index reflects the soil structural condition based on the slope of the soil water retention curve at its inflection point [40] and therefore represents the pore size distribution and depends basically on microstructural porosity [40]. Thus, NF, due to its lower clay content and higher stoniness (Tables 1, 3), compromised the microstructural porosity, culminating in lower S Index. Except in the NF, the soil was considered of good physical quality (S Index > 0.35) [40]. It is noteworthy that the NF is in a different soil type from other areas (Inceptisol).

The soil water retention curve for the NF and ER areas had similar behavior, with gradual decrease in the pore diameter, and lower water retention capacity. On the other hand, the NR, GA, and RF areas have changed more abruptly from large pores to small pores, and greater water retention capacity (Fig. 2). These results may be due to the lower clay content and higher stoniness of NF and ER areas (Tables 1, 3).

The RF had greater available water capacity than the NF, especially due to the clay content and stoniness. Post-mining areas did not differ for the soil properties AWC_{INFL} and θ_{INFL} , but for AWC, ER was smaller. After post-mining reclamation process, changes occur in soil physical properties related to pore size distribution, basically reducing macropores and increasing micropores, which occur few

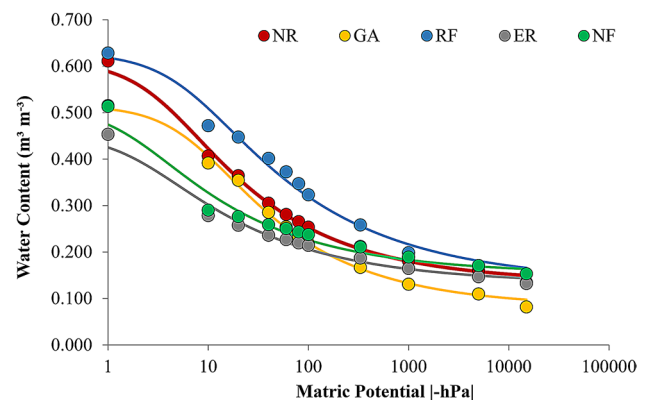


Fig. 2 Soil water retention curves in areas affected iron ore mining and native vegetation in the Serra do Curral Municipal Park and Fort Lauderdale Park, Minas Gerais State, Brazil. NR=natural revegetation; GA=gully area; RF=rupestrian field; NF=native forest; ER=eucalyptus revegetation

years after recovery [20]. However, our results contrast with Barros et al. [20], since NR improved soil aeration function (Table 3). This finding suggests that reclamation process for long years leads to improvements in soil physical quality in iron ore mining areas.

In addition to the problem of low water retention and availability, mining areas often have heavy metal contamination and deteriorating water quality [54]. However, this aspect was not the subject of this study, and further research in this matter is recommended.

3.3 Visual soil assessment

The visual analysis showed no difference for structure and the presence of mottling in the soil. There was a low presence of earthworms in the areas, and therefore, the related data were not discussed in this paper. Greater ground cover was observed for the NF area compared to the NR and GA areas. As for plant cover, the area with greater plant contribution, NF, visually presented greater soil coverage, thus enabling good soil quality [47]. Regarding the color attribute, the NF and RF areas did not differ. The NF, RF, and ER areas did not differ in their total porosity, with the highest values, and NR and GA with the lowest values. The relief with a more stable topography and, therefore, with less difficulty of transit is in the NF and the most unstable of the GA (Table 4). The more human-affected areas (NR and GA) showed a structure more susceptible to disaggregation, being visually more degraded and eroded due to the lower plant cover and SOM [55].

The visual index of the NR and GA was smaller than the others, being classified as of poor soil quality. The areas of NF, RF, and ER were classified as of moderate soil quality (Table 5). The VSA is a technique widely used in agricultural and pasture areas [16, 56–58], and this is one of the rare studies conducted in mined areas. The GA and NR are in an advanced degree of degradation and, therefore, fall into

Table 4 Values from soil visual analysis in areas affected by iron ore mining and native vegetation in the Serra do Curral Municipal Park and Fort Lauderdale Park, Minas Gerais State, Brazil

Visual analysis	NR	GA	RF	NF	ER
Ground cover	0.333c	0.166c	0.833b	1.833a	1.000b
Color	0.833b	1.000b	1.833a	1.833a	1.166b
Structure	1.166a	1.000a	1.000a	1.166a	1.500a
Mottled	1.000a	0.666a	1.333a	1.833a	1.333a
Total porosity	0.666b	0.666b	1.833a	1.833a	1.333a
Surface relief	0.833c	0.166d	1.333b	2.000a	1.333b

*Means followed by the same letter in the row do not differ at the 5% level of significance by the Scott–Knott test. NR=natural revegetation; GA=gully area; RF=rupestrian field; NF=native forest; ER=eucalyptus revegetation

Table 5 Soil quality index values and their classification, according to Shepherd (2000), in areas affected by iron ore mining and native vegetation in the Serra do Curral Municipal Park and Fort Lauderdale Park, Minas Gerais State, Brazil

Site	Visual index	Classification
NR	9b	Poor
GA	8.5b	Poor
RF	19a	Moderate
NF	14a	Moderate
ER	15.5a	Moderate

Means followed by the same letter in the column do not differ at the 5% level of significance by the Scott–Knott test. NR=natural revegetation; GA=gully area; RF=rupestrian field; NF=native forest; ER=eucalyptus revegetation

the "poor" quality category [16]. However, the other areas were classified as having moderate visual quality, possibly because they already had better plant cover and/or because the analysis was influenced by the high stoniness found. The visual evaluation is useful to quickly estimate the attributes of an agricultural soil. However, in a more comprehensive characterization, it is necessary to make use of the largest number of possible laboratory analyses.

3.4 Distinction of environments through physical attributes

The soil physical properties were sensitive to differentiate the evaluated areas, using PCA (Fig. 3). The first three principal components (PCs) accumulated approximately 70% of the data variance. The percentage of variance captured by PCA greater than 60% indicates good explanation for any phenomenon studied [59].

Soil physical properties are more correlated with PC1, and therefore, contributions were: Pd (0.60), stoniness (0.64), SOM (0.60), Bd (0.83), MWD (0.91), GMD (0.89), ASI (0.80), SSI (0.71), S Index (−0.85), and AWC (−0.69). The clay content (0.76), SOM (0.60), PWP (0.61), ACb (0.64), θ_{INFL} (0.81), and AWC_{INFL} (0.74) had most correlations with PC2. The Mac (0.93), RFC (−0.89), and E_1 (0.65) had most correlations with PC3. Silt and sand contents, FC, and FI had low correlation in these PCs, indicating little importance to distinguish the areas (Table 6). PCs can be used to reduce the original variables to a smaller number of new variables (PC) by explaining most of the variation in the original variables [60], therefore serving as an important tool that provides a minimum dataset for environmental monitoring [13].

Figure 3 shows the observations projections and coordinates of variables. PC1 (33%) and PC2 (22%) distinguished three environments: (1) GA; (2) NR and RF; and (3) ER and NF. These two PCs summarize the soil physical properties

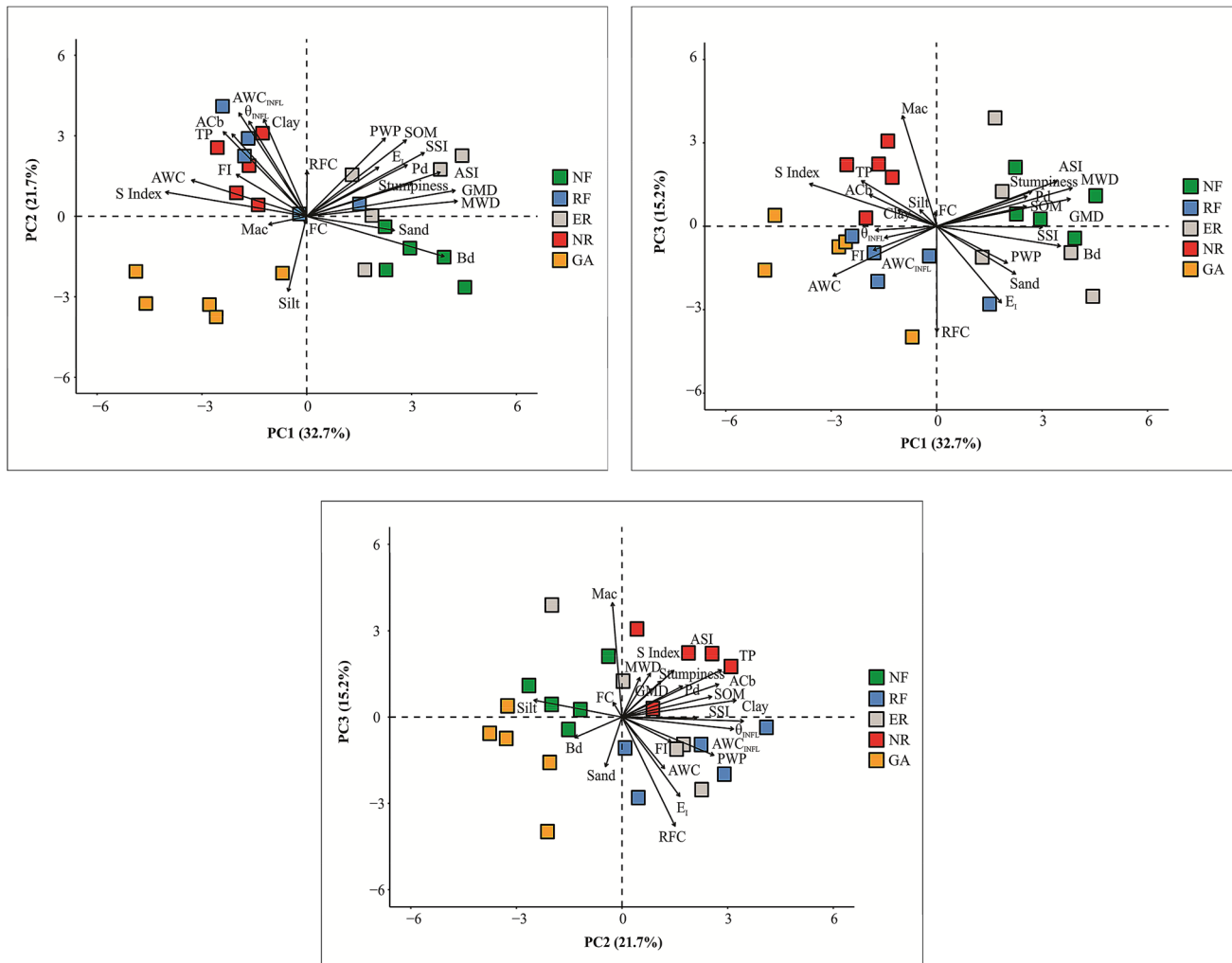


Fig. 3 Projections observations and coordinates of soil physical properties in areas affected iron ore mining and native vegetation in the Serra do Curral Municipal Park and Fort Lauderdale Park,

Minas Gerais State, Brazil. NR=natural revegetation; GA=gully area; RF=rupestrian field; NF= native forest; ER=eucalyptus revegetation

related to soil aggregation, soil porosity, and water availability to plants. The PC1 (33%) x PC3 (15%) and PC2 (22%) x PC3 (15%) biplots best distinguish the NR area from the RF. This was due to higher Mac and lower RFC, high correlation with PC3, in NR compared to the RF, which confirmed the analysis of variance (ANOVA) (Table 3). These results show mining activity impact remains on rupestrian field—that was once a mining area (NR)—regarding soil physical quality, measured by aeration soil function.

GA is almost always associated with accelerated erosion and therefore with instability in the landscape [61] post-mining, being an area with the highest level of degradation. GA presented higher silt content and lower SOM (Fig. 3, Table 3), which have a strong influence on soil erodibility [62]. The NR and RF areas suffer from laminar erosion

process (visual field evaluation); however, soil attributes, landscape, and vegetation cover prevent a gully erosion process. These areas were grouped by higher clay content, soil porosity, and available water capacity. Therefore, NR, over 36 years, has been able to recover these soil physical properties, mainly related to soil water availability function.

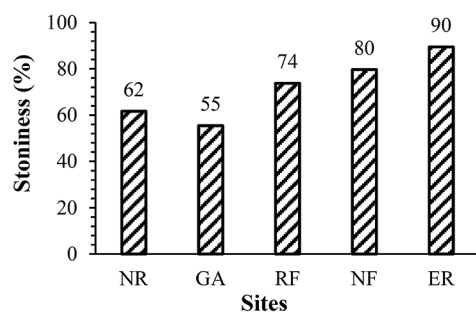
The ER area approached the condition of NF, with higher SOM and soil aggregation attributes (Fig. 3, Table 3). These results indicate that eucalyptus cultivation in the recovery of post-mining areas in a rupestrian field environment improves the soil physical properties rather than natural revegetation and even the rupestrian field condition. Eucalyptus can be used in the reclamation of areas affected by iron ore mining, being a species that exhibit

Table 6 Principal component analysis of the soil physical properties in areas affected by iron ore mining and native vegetation in the Serra do Curral Municipal Park and Fort Lauderdale Park, Minas Gerais State, Brazil

Variables	PC 1	PC 2	PC3
Particle density (kg dm ⁻³)	0.60	0.40	0.25
Clay (%)	-0.26	0.76	0.14
Silt (%)	-0.11	-0.59	0.14
Sand (%)	0.53	-0.11	-0.40
Stoniness (%)	0.64	0.26	0.29
Soil organic matter (%)	0.60	0.60	0.17
Bulk density (kg dm ⁻³)	0.83	-0.31	-0.17
Total porosity (m ³ m ⁻³)	-0.50	0.66	0.38
Macroporosity (m ³ m ⁻³)	-0.23	-0.06	0.93
Relative field capacity	0.00	0.35	- 0.89
Permanent wilting point (m ³ m ⁻³)	0.47	0.61	-0.31
Field capacity (m ³ m ⁻³)	-0.01	-0.06	0.12
Air capacity (m ³ m ⁻³)	-0.45	0.64	0.27
Mean weighted Diameter (mm)	0.91	0.12	0.32
Geometric mean Diameter (mm)	0.89	0.20	0.23
Flocculation index (%)	-0.42	0.33	-0.20
Aggregate stability index (%)	0.80	0.34	0.38
Structural stability index (%)	0.71	0.50	-0.01
S Index	- 0.85	0.19	0.36
Available water capacity (m ³ m ⁻³)	- 0.69	0.28	-0.42
Integral energy (kg J ⁻¹)	0.43	0.38	- 0.65
θ _{INFL} (m ³ m ⁻³)	-0.41	0.81	-0.03
Available water capacity _{INFL} (m ³ m ⁻³)	-0.35	0.74	-0.10
Percentage of variance explained (%)	32.71	21.70	15.15

Loads larger than 0.60 are shown in bold type and show the differential importance of the variables in each component. Total variance of the model explained by the first three components: 69.56%

high survival and growth [63, 64]. Native vegetation may be more difficult to grow than exotic species [64], especially when the natural vegetation is composed of shrubs and some sparse grasses, such as the rupestrian fields.



The soil stoniness was higher in the ER area (90%) and smaller in the GA and NR areas (60%) (Fig. 4a). The areas with higher percentage of stones had a greater percentage of aggregates of 8–2 mm (Fig. 4b), showing significant correlation. It is important to highlight that soil aggregation attributes were strongly influenced by high soil stoniness (Figs. 4b, 5). Areas with higher SSI, ASI, MWD, and GMD had higher stoniness (Fig. 4a), so many aggregates are stones, which biased some soil aggregates attributes. However, the SSI attribute is determined from the SOM, silt, and clay content of the sample, not influenced by soil stoniness. In addition, SOM, a fundamental property for soil aggregation [65], was highly correlated with soil aggregation attributes (Fig. 5). Therefore, it is suggested that the methodology for determining aggregate stability be adapted to conditions of high soil stoniness, as usually occurs in post-mining areas, or use indirect indicators like SSI.

Soil properties related to soil aggregation, soil porosity, and water availability had a distinct correlation with Bd and S Index. Bd had a positive correlation with soil aggregation and a negative correlation with porosity and water available capacity; the opposite was observed for the S Index. Areas with higher soil aggregation showed higher stoniness and Pd and, therefore, higher Bd. The S Index is an indicator of physical soil quality [40]; therefore, a positive correlation with soil aggregation is to be expected, but most soil aggregation indicators were biased by soil stoniness, causing a negative correlation with S Index.

Soil characteristics like clay content and Pd have some influence on soil properties (Fig. 5) which can be explained due to pedological/soil genesis variation in the evaluated area (Inceptisol to Entisol). Clay content correlated positively with TP and ACb. The correlation of the clay content with the available water capacity depended on the criterion adopted to estimate the field capacity. AWC_{INFL} possibly correlates due to more water retention in clayey soil [38]. Pd basically influences soil aggregation attributes as

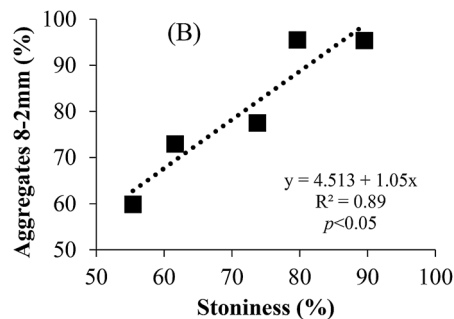


Fig. 4 Mean values of stoniness (%) (a) and linear regression between the aggregates 8–2 mm and stoniness (b), in areas affected iron ore mining and native vegetation in the Serra do Curral Municipal Park and Fort Lauderdale Park, Minas Gerais State, Brazil. NR=natural revegetation; GA=gully area; RF=rupestrian field; NF=native forest; ER=eucalyptus revegetation

ral Municipal Park and Fort Lauderdale Park, Minas Gerais State, Brazil. NR=natural revegetation; GA=gully area; RF=rupestrian field; NF=native forest; ER=eucalyptus revegetation

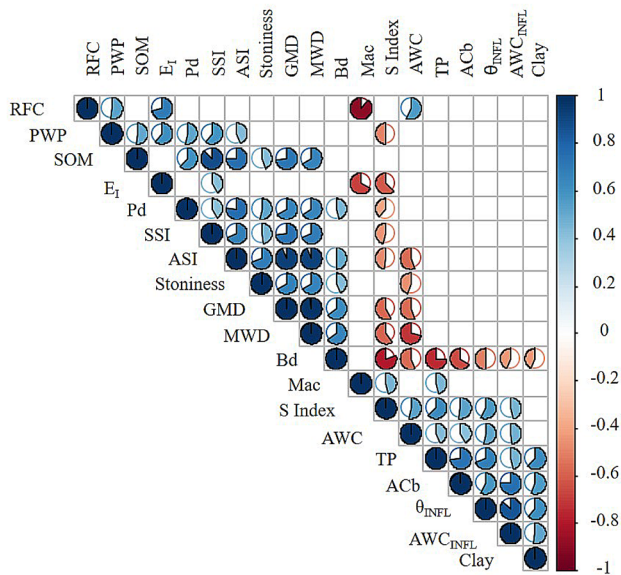


Fig. 5 Pearson correlation coefficient of soil physical properties in areas affected iron ore mining and native vegetation in the Serra do Curral Municipal Park and Fort Lauderdale Park, Minas Gerais State, Brazil. Pies indicate significant correlation ($p < 0.05$)

shown above. However, stoniness had more impact on soil properties because it reflects mining reclamation process [20] and therefore is essential in interpreting soil functions affected by mining.

Considering the contribution of the studied variables (eigenvector) to the main components, the soil physical properties most sensitive to the recovery processes of post-mining areas were: Mac, RFC, GMD, and MWD. Thus, the soil aggregates stability and soil aeration capacity can be used for the diagnosis and monitoring of post-iron ore mining areas.

4 Conclusion

Iron ore mining process impacts soil physical quality measured through porosity and aggregation properties and therefore could impact ecosystems services. Erosion risk evaluated by aggregate stability increased in an area without reclamation intervention culminating in a gully erosion (GR). The texture and stoniness variations were related to the aggregation and pore size distribution indicators, which biased results of some physical indicators and must be considered, for example in the interpretation of the results of Bd and S Index. The soil physical properties most sensitive to the recovery processes of post-mining areas were: Mac, RFC, GMD, and MWD.

Natural revegetation (NR) shows high erosion risk inferred through aggregation indicators, despite similar SOM content and higher plant-available water and air compared with NF. Moreover, soil and water conservation practices should be employed to stabilize and recover soil quality. Nevertheless, eucalyptus revegetation (ER) proved to be more effective in reclamation areas degraded by iron ore mining compared to NR. ER enhanced soil organic matter content and therefore had similar soil structure stability compared to NF as well as most of porosity indicators.

Our hypothesis was partially proved, since VSA alone was not able to characterize the soil physical quality, mainly in the post-mining areas, because it was designed for agricultural soils. Future work should explore relation between soil physical properties and VSA in post-mining areas.

References

- Shrestha RK, Lal R (2011) Changes in physical and chemical properties of soil after surface mining and reclamation. *Geoderma* 161:168–176. <https://doi.org/10.1016/j.geoderma.2010.12.015>
- Dorgbetor WHK, Dowuona GNN, Danso SKA, Amatekpor JK, Ogunkunle AO, Boateng E (2012) evaluation of quality of some rehabilitated mined soils within the AngloGold-Ashanti Concession in Ghana. *Int J Geosci* 3:50–61. <https://doi.org/10.4236/ijg.2012.31007>
- Yan D, Zhao F, Sun OJ (2013) Assessment of vegetation establishment on tailings dam at an iron ore mining site of suburban Beijing, China, 7 years after reclamation with contrasting site treatment methods. *Environ Manag* 52:748–757. <https://doi.org/10.1007/s00267-013-0092-y>
- Masto RE, Sheik S, Nehru G, Selvi VA, George J, Ram LC (2015) Assessment of environmental soil quality around Sonepur Bazar mine of Raniganj coalfield, India. *Solid Earth* 6:811–821. <https://doi.org/10.5194/se-6-811-2015>
- Milder AI, Fernández-Santos B, Martínez-Ruiz C (2013) Colonization patterns of woody species on lands mined for coal in Spain: preliminary insights for forest expansion. *Land Degrad Dev* 24:39–46. <https://doi.org/10.1002/ldr.1101>
- Moebius-Clune BN, van Es HM, Idowu OJ, Schindelbeck RR, Kimetu JM, Ngoze S, Lehmann J, Kinyangi JM (2011) Long-term soil quality degradation along a cultivation chronosequence in western Kenya. *Agr Ecosyst Environ* 141:86–99. <https://doi.org/10.1016/j.agee.2011.02.018>
- Longo RM, Ribeiro AI, De Melo WJ (2011) Recuperação de solos degradados na exploração mineral de cassiterita: Biomassa microbiana e atividade da desidrogenase. *Bragantia* 70:132–138. <https://doi.org/10.1590/S0006-87052011000100019>
- Shrestha RK, Lal R (2006) Ecosystem carbon budgeting and soil carbon sequestration in reclaimed mine soil. *Environ Int* 32:781–796. <https://doi.org/10.1016/j.envint.2006.05.001>
- Seybold CA, Grossman RB, Sinclair HR, McWilliams KM, Struben GR, Wade SL (2004) Evaluating soil quality on reclaimed coal mine soils in Indiana. In: Proceedings of the 2004 national meeting of the American Society of Mining and Reclamation and the 25th West Virginia Surface Mine Drainage Task Force, American Society of Mining and Reclamation, Lexington, KY. pp 1644–1663

10. Guebert MD, Gardner TW (2001) Macropore flow on a reclaimed surface mine: infiltration and hillslope hydrology. *Geomorphology* 39:151–169. [https://doi.org/10.1016/S0169-555X\(00\)00107-0](https://doi.org/10.1016/S0169-555X(00)00107-0)
11. Akala VA, Lal R (2001) Soil organic pools and sequestration rates in reclaimed minesoils in Ohio. *J Environ Qual* 30:2090–2104
12. Ganjegunte GK, Wick AF, Stahl PD, Vance GF (2009) Accumulation and composition of total organic carbon in reclaimed coal mine lands. *Land Degrad Dev* 20:156–175. <https://doi.org/10.1002/ldr.889>
13. Rinot O, Levy GJ, Steinberger Y, Svoray T, Eshel G (2019) Soil health assessment: a critical review of current methodologies and a proposed new approach. *Sci Total Environ* 648:1484–1491. <https://doi.org/10.1016/j.scitotenv.2018.08.259>
14. Pond GJ, Passmore ME, Pointon ND, Felbinger JK, Walker CA, Krock KJG, Fulton JB, Nash WL (2014) Long-term impacts on macroinvertebrates downstream of reclaimed mountaintop mining valley fills in Central Appalachia. *Environ Manag* 54:919–933. <https://doi.org/10.1007/s00267-014-0319-6>
15. Bünemann EK, Bongiorno G, Bai Z, Creamer RE, De Deyn G, Goede R, Fleskens L, Geissen V, Kuyper TW, Mäder P, Pulleman M, Sukkel W, van Groenigen JW, Brussaard L (2018) Soil quality – a critical review. *Soil Biol Biochem* 120:105–125. <https://doi.org/10.1016/j.soilbio.2018.01.030>
16. Shepherd TG (2000) Visual soil assessment: Field guide for cropping and pastoral grazing on flat to rolling country. Horizons. mw & Landcare Research. 84 p
17. Niero LAC, Dechen SCF, Coelho RM, De Maria IC (2010) Avaliações visuais como índice de qualidade do solo e sua validação por análises físicas e químicas em um latossolo vermelho distrófico com usos e manejos distintos. *Rev Bras Ciênc Solo* 34:1271–1282. <https://doi.org/10.1590/S0100-06832010000400025>
18. Carvalho RPB (2011) Contributions of geosystems analysis in the recovery of areas degraded by mining activities. *Caderno de Geografia* 21:13–28
19. Vicq R, Matschullat J, Leite MGP, Nalini Junior HA, Mendonça FPC (2015) Iron Quadrangle stream sediments, Brazil: geochemical maps and reference values. *Environ Earth Sci* 74:4407–4417. <https://doi.org/10.1007/s12665-015-4508-2>
20. Barros DA, Pereira JAA, Ferreira MM, Silva BM, Ferreira Filho D, Nascimento GO (2013) Soil physical properties of high mountain fields under bauxite mining. *Cienc Agrotec* 37:419–426. <https://doi.org/10.1590/S1413-70542013000500005>
21. Alvares CA, Stape JL, Sentelhas PC, Gonçalves JLM, Sparovek G (2013) Köppen's climate classification map for Brazil. *Meteorol Z* 22:711–728. <https://doi.org/10.1127/0941-2948/2013/0507>
22. Carvalho Filho A, Curi N, Shinzato E (2010) Relações solo-paisagem no Quadrilátero Ferrífero em Minas Gerais. *Pesq Agropec Bras* 45:903–916. <https://doi.org/10.1590/S0100-204X2010000800017>
23. Vasconcelos MF (2011) O que são campos rupestres e campos de altitude nos topos de montanha do leste do Brasil? *Braz J Bot* 34:241–246. <https://doi.org/10.1590/S0100-84042011000200012>
24. Brasil (1983) Ministério das Minas e Energia. Projeto RADAM Brasil. Folhas SF. 23/24 Rio de Janeiro/Vitória: geologia, geomorfologia, pedologia, vegetação e uso potencial da terra. Rio de Janeiro: DNPM
25. Morellato LPC, Haddad CFB (2000) Introduction: the brazilian atlantic forest. *Biotropica* 32:786–792
26. Myers N, Mittermeier RA, Mittermeier CG, Fonseca GAB, Kent J (2000) Biodiversity hotspots for conservation priorities. *Nature* 403:853–858. <https://doi.org/10.1038/35002501>
27. Blake GR, Hartge K (1986) Particle density. In: Klute A (ed) *Methods of soil analysis: physical and mineralogical methods*, part 1. American Society of Agronomy, Madison, pp 377–382
28. Teixeira WG, Donagemma GK, Wenceslau AF, Teixeira G (2017) *Manual de métodos de análise de solos*. Embrapa Solos, Rio de Janeiro, p 573p
29. Castro Filho C, Muzilli O, Podanoschi AL (1998) Estabilidade dos Agregados e sua relação com o teor de carbono orgânico num latossolo roxo distrófico, em função de sistemas de plantio, rotações de culturas e métodos de preparo das amostras. *Rev Bras Ciênc Solo* 22:527–538. <https://doi.org/10.1590/S0100-06831998000300019>
30. Silva EA, Oliveira GC, Carducci CE, Silva BM, Oliveira LM, Costa JC (2013) Increasing doses of agricultural gypsum, aggregate stability and organic carbon in Cerrado Latosol under Coffee crop. *Revista de Ciências Agrárias* 56:25–32. <https://doi.org/10.4322/rca.2013.012>
31. Reynolds WD, Drury CF, Yang XM, Fox CA, Tan CS, Zhang TQ (2007) Land management effects on the near-surface physical quality of a clay loam soil. *Soil Tillage Res* 96:316–330. <https://doi.org/10.1016/j.still.2007.07.003>
32. Grohmann F (1960) Análise de agregados de solos. *Bragantia* 19:201–213. <https://doi.org/10.1590/S0006-87051960000100013>
33. van Genuchten MT (1980) A closed-form equation for predicting the hydraulic conductivity of unsaturated soils. *Soil Sc Soc Am J* 44:892–898
34. Klein VA (2014) Física do solo. EDIUPF, Passo Fundo
35. Reynolds WD, Drury CF, Yang XM, Tan CS (2008) Optimal soil physical quality inferred through structural regression and parameter interactions. *Geoderma* 146:466–474. <https://doi.org/10.1016/j.geoderma.2008.06.017>
36. Dexter AR, Bird NRA (2001) Methods for predicting the optimum and the range of soil water contents for tillage based on the water retention curve. *Soil Tillage Res* 57:203–212. [https://doi.org/10.1016/S0167-1987\(00\)00154-9](https://doi.org/10.1016/S0167-1987(00)00154-9)
37. Ferreira MM, Marcos ZZ (1983) Estimativa da capacidade de campo de Latossolo Roxo distrófico e Regossolo através do ponto de inflexão da curva característica de umidade. *Ciência e Prática* 7:96–101
38. Silva BM, Silva EA, Oliveira GC, Ferreira MM, Serafim ME (2014) Plant-available soil water capacity: Estimation methods and implications. *Rev Bras Ciênc Solo* 38:464–475. <https://doi.org/10.1590/S0100-06832014000200011>
39. Asgarzadeh H, Mosaddeghi MR, Nikbakht AM (2014) SAWCal: A user-friendly program for calculating soil available water quantities and physical quality indices. *Comput Electron Agric* 109:86–93. <https://doi.org/10.1016/j.compag.2014.09.008>
40. Dexter AR (2004) Soil physical quality Part I. Theory, effects of soil texture, density, and organic matter, and effects on root growth. *Geoderma* 120:201–214. <https://doi.org/10.1016/j.geoderma.2003.09.004>
41. R Core Team (2014) R: a language and environment for statistical computing. R Foundation for Statistical Computing, Vienna, Austria. <https://www.R-project.org/>
42. Boix-Fayos C, Calvo-Cases A, Imeson AC, Soriano-Soto MD (2001) Influence of soil properties on the aggregation of some Mediterranean soils and the use of aggregate size and stability as land degradation indicators. *CATENA* 44:47–67. [https://doi.org/10.1016/S0341-8162\(00\)00176-4](https://doi.org/10.1016/S0341-8162(00)00176-4)
43. Shrestha BM, Singh BR, Sitaula BK, Lal R, Bajracharya RM (2007) Soil aggregate-and particle-associated organic carbon under different land uses in Nepal. *Soil Sci Soc Am J* 71:1194–1203. <https://doi.org/10.2136/sssaj2006.0405>
44. Spohn M, Giani L (2011) Impacts of land use change on soil aggregation and aggregate stabilizing compounds as

- dependent on time. *Soil Biol Biochem* 43:1081–1088. <https://doi.org/10.1016/j.soilbio.2011.01.029>
45. Adesodun JK, Olowokere FA, Soretire AA, Adejuyigbe CO, Adewole AO, Akintokun PO, Omuju OJ (2015) Carbon-nitrogen stocks and structural stability of a tropical loamy sand soil as influenced by *Tithonia diversifolia* (L.) and other fertilizers. *Int J Soil Sci* 10:37–44. <https://doi.org/10.3923/ijss.2015.37.44>
46. Yang F, Zhang GL, Yang JL, Li DC, Zhao YG, Liu F, Yang RM, Yang F (2014) Organic matter controls of soil water retention in an alpine grassland and its significance for hydrological processes. *J Hydrol* 519:3086–3093. <https://doi.org/10.1016/j.jhydrol.2014.10.054>
47. Plaza C, Courtier-Murias D, Fernández JM, Polo A, Simpson AJ (2013) Physical, chemical, and biochemical mechanisms of soil organic matter stabilization under conservation tillage systems: A central role for microbes and microbial by-products in C sequestration. *Soil Biol Biochem* 57:124–134. <https://doi.org/10.1016/j.soilbio.2012.07.026>
48. Six J, Paustian K (2014) Aggregate-associated soil organic matter as an ecosystem property and a measurement tool. *Soil Biol Biochem* 68:4–9. <https://doi.org/10.1016/j.soilbio.2013.06.014>
49. Dlapa P, Chrenková K, Mataix-Solera J, Šimkovic I (2012) Soil profile improvement as a by-product of gully stabilization measures. *CATENA* 92:155–161. <https://doi.org/10.1016/j.catena.2011.12.002>
50. Tisdall JM, Oades JM (1982) Organic-matter and water-stable aggregates in soils. *Eur J Soil Sci* 33:141–163. <https://doi.org/10.1111/j.1365-2389.1982.tb01755.x>
51. Degens BP, Sparling GP, Abbott LK (1994) The contribution from hyphae, roots and organic-carbon constituents to the aggregation of a sandy loam under long-term clover-based and grass pastures. *Eur J Soil Sci* 45:459–468. <https://doi.org/10.1111/j.1365-2389.1994.tb00531.x>
52. Zhang L, Jinmanwang W, Bai Z, Chunjuan LV (2015) Effects of vegetation on runoff and soil erosion on reclaimed land in an opencast coal-mine dump in a loess area. *CATENA* 128:44–53. <https://doi.org/10.1016/j.catena.2015.01.016>
53. White RE (2006) Principles and practice of soil science, 4th edn. Blackwell Publishing, Oxford, UK
54. Shahmoradi B, Hajimirzaei S, Amanollahi J, Wantalla K, Maleki A, Lee S, Shim MJ (2020) Influence of iron mining activity on heavy metal contamination in the sediments of the Aqyazi River. *Iran Environ Monit Assess* 192:521. <https://doi.org/10.1007/s10661-020-08524-7>
55. Rocha JH, Santos AJM, Diogo FA, Backes C, Melo AGC, Borelli K, Godinho TO (2015) Reflorestamento e Recuperação de Atributos Químicos e Físicos do Solo. *Floresta e Ambiente* 22:299–306. <https://doi.org/10.1590/2179-8087.041613>
56. Mueller L, Kay BD, Hu C, Li Y, Schindler U, Behrendt A, Shepherd TG, Ball BC (2009) Visual assessment of soil structure: Evaluation of methodologies on sites in Canada, China and Germany: Part I: comparing visual methods and linking them with soil physical data and grain yield of cereals. *Soil Tillage Res* 103:178–187. <https://doi.org/10.1016/j.still.2008.12.015>
57. Guimarães RML, Ball BC, Tormena CA (2011) Improvements in the visual evaluation of soil structure. *Soil Use Manag* 27:395–403. <https://doi.org/10.1111/j.1475-2743.2011.00354.x>
58. Murphy BW, Crawford MH, Duncan DA, McKenzie DC, Koen TB (2013) The use of visual soil assessment schemes to evaluate surface structure in a soil monitoring program. *Soil Tillage Res* 127:3–12. <https://doi.org/10.1016/j.still.2012.06.003>
59. Stangl DK (2008) Encyclopedia of statistics in behavioral science. *J Am Stat Assoc* 103:881–882. <https://doi.org/10.1198/jasa.2008.s230>
60. Jolliffe IT, Cadima J (2016) Principal component analysis: a review and recent developments. *Philos Trans R Soc A* 374:20150202. <https://doi.org/10.1098/rsta.2015.0202>
61. Morgan RPC (2005) Soil erosion and conservation, 3rd edn. Blackwells, Oxford, p 304
62. Wischmeier WH, Mannering JV (1969) Relation of soil properties to its erodibility. *Soil Sci Soc Am Pro* 33:131–137
63. Hiremath KG (2003) Recent advances in environmental science. Discovery Publishing House, Delhi
64. Brusseau M, Pepper I, Gerba C (2019) Environmental and pollution science, 3rd edn. Elsevier, Amsterdam
65. Six J, Bossuyt H, Degryze S, Denef K (2004) A history of research on the link between (micro) aggregates, soil biota, and soil organic matter dynamics. *Soil Tillage Res* 79:7–31. <https://doi.org/10.1016/j.still.2004.03.008>

Publisher's Note Springer Nature remains neutral with regard to jurisdictional claims in published maps and institutional affiliations.